ROYAL SOCIETY
OF CHEMISTRY

PAPER

Check for updates

A novel CRISPR-Cas12a-based diagnostic for rapid and highly sensitive detection of West Nile virus

Asli Erol,†[a] Dilan Celebi-Birand, [iD]†[a] Ebru Yilmaz,[a] Ceylan Polat, [iD][b]
Ozge Erisoz Kasap,[c] Bulent Alten[c] and Memed Duman [iD] *[a]

Climate change is increasing the global threat of vector-borne diseases, including West Nile Virus (WNV), a significant human and animal pathogen transmitted primarily by *Culex* mosquitoes. Current WNV diagnostic methods, while including sensitive techniques like RT-PCR, have limitations in early detection, practicality, and cost-effectiveness. There is an urgent need to develop novel and more efficient strategies to address these challenges and to facilitate the surveillance and management of WNV infections and their spread. This study presents a highly specific and sensitive CRISPR-Cas12a-based detection protocol for WNV detection. Through systematic analysis of key reaction parameters (time: 0–60 min; reporter concentration: 1–80 nM, Cas12a and crRNA concentration: 5.625–90 nM; and template amount: 10^{-2}–10^5 pg) and integration with reverse transcriptase recombinase polymerase amplification to enhance sensitivity through an isothermal technique, this assay demonstrates a novel strategy for the rapid detection of WNV, achieving 10 femtomolar sensitivity within one hour. Moreover, the assay retained its efficacy at different temperatures (25 °C and 37 °C) and in biological matrices containing the host (fly or human) genetic material, which supports its applicability in resource-limited settings. Therefore, the method presented here has the potential for broad application in diverse point-of-care settings for rapid diagnosis of WNV.

Introduction

Climate change is anticipated to impact the prevalence of vector-borne diseases significantly. Rising temperatures and shifts in precipitation patterns are projected to facilitate the expansion of vector species (*e.g.*, mosquitoes, sandflies, fleas, and ticks) into previously unaffected regions, thereby exposing resident populations to a spectrum of diseases, including malaria, dengue, Zika virus disease, and West Nile fever.[1,2] Moreover, these changes can significantly impact vector abundance and accelerate the development of pathogens within vectors, potentially enhancing their virulence or reducing the incubation period, and present a challenge to the effective prevention and control of vector-borne diseases.[3,4] Consequently, it is critical to develop novel strategies to detect vectors *in situ* with high sensitivity and specificity, while simultaneously being user-friendly and cost-effective.

Orthoflavivirus nilense (West Nile virus – WNV) is a member of the *Orthoflavivirus* genus, which contains other significant human pathogens such as *Orthoflavivirus zikaense* (Zika virus), *Orthoflavivirus denguei* (Dengue virus), and *Orthoflavivirus flavi* (Yellow fever virus). Primarily transmitted by *Culex* mosquitoes, WNV infection manifests with a spectrum of clinical outcomes, ranging from mild fever to severe neurological complications such as encephalitis and meningitis, with fatal cases reported.[5] WNV exhibits significant neurotropism, with clinical symptoms reflecting its impact on the central nervous system. Histopathological studies further revealed that WNV causes characteristic lesions, including neuronophagia, microglial nodules, and perivascular inflammation, primarily in the thalamus, basal ganglia, brainstem, and spinal cord.[6] Since its initial discovery, WNV has emerged as a global health concern, causing recurrent outbreaks across all continents. The economic impact of WNV is substantial, including the costs of patient care, disease control programs, and losses within the livestock and agricultural sectors. The limitations of existing antiviral treatments and the lack of effective vaccines exacerbate the disease burden and contribute to the persistent occurrence of outbreaks in both endemic and non-endemic regions. Notably, a marked increase in human cases has been observed over the past two decades in Europe, starting with a significant 1996 Romanian outbreak of 393 human cases, leading to annual summer

[a] *Institute of Science, Nanotechnology and Nanomedicine Division,*
Hacettepe University, Ankara, Turkey. E-mail: memi@hacettepe.edu.tr
[b] *Department of Medical Microbiology, Faculty of Medicine, Hacettepe University,*
Ankara, Turkey
[c] *Department of Biology, Ecology Division, VERG Labs, Hacettepe University,*
Ankara, Turkey
† The authors have contributed equally to this work.

outbreaks across the continent. Following its 1999 introduction to North America, the USA alone recorded over 55 000 WNV cases by 2021.[5,7] WNV infection, therefore, poses a significant threat to public and animal health due to its potential to cause unpredictable and widespread epidemics.[8]

Current diagnostic approaches for WNV infection include enzyme-linked immunosorbent assays (ELISAs),[9] immunohistochemistry,[10] viral culture,[11] and nucleic acid amplification tests (NAATs).[12] Among these, ELISA-based assays detect anti-WNV antibodies in serum. However, during the initial acute stage of the infection, there is a serological window period when antibodies are not detectable, making serological tests unreliable.[9] Furthermore, antibody cross-reactivity among flaviviruses presents a significant challenge in serological analyses.[13] Detection of a WNV antigen *via* immunohistochemical analysis requires brain tissue biopsy, limiting its applicability to post-mortem investigations. Viral culture, a sensitive but time-consuming technique, involves isolating the virus from biological specimens such as blood, cerebrospinal fluid (CSF), or brain tissue obtained through biopsy or autopsy. Successful viral isolation necessitates specialised expertise in handling of orthoflaviviruses and access to a biosafety level 3 containment facility.[11] NAATs, such as reverse transcription polymerase chain reaction (RT-PCR), are employed to detect the presence of the WNV genetic material in blood or other body fluid specimens.[12,14] In recent years, RT-PCR has emerged as the gold standard for the diagnosis of numerous viral infections due to its standardised format, reproducibility, sensitivity and specificity.[15] While being highly reliable, NAATs may exhibit limitations in detecting the virus during the early stages of infection. Furthermore, the use of high primer concentrations (*e.g.*, 0.6 μM) and stringent control of experimental conditions is required, as well as preventing contamination to avoid false-positive results.[14] Finally, in the context of most orthoflavivirus-associated diseases, the routine application of qRT-PCR on serum, plasma, and CSF samples faces limitations due to the short duration and low levels of viremia, presenting false-negative results.[15]

Despite their limitations, with further refinement, NAATs may offer high sensitivity, specificity, speed, and cost-effectiveness. Among the emerging NAATs, the CRISPR-Cas systems, particularly Cas12a, exhibit considerable promise and offer several distinct advantages as a diagnostic tool. Cas12a, also known as Cpf1, is a single RNA-guided endonuclease that utilises a T-rich protospacer-adjacent motif (PAM) to recognise its target, and cleaves DNA through the generation of staggered double-stranded breaks, thereby enabling versatile targeting capabilities.[16] This unique characteristic, coupled with Cas12a's inherent high specificity in DNA targeting, minimises the risk of off-target effects.[17] Cas12a also exhibits a remarkable potential for sensitive and specific detection of nucleic acids due to the unique indiscriminate single-stranded DNA (ssDNA) cleavage activity (*i.e.*, *trans*-cleavage).[18,19] The *trans*-cleavage of ssDNA serves as a signal amplification mechanism, significantly enhancing assay sensitivity.[20] Various reporter systems, including fluorescent probes, colorimetric indicators, and

lateral flow assays, can be employed to detect Cas12a activity. Furthermore, Cas12a, similar to other CRISPR-Cas systems, demonstrates high target specificity, minimising the risk of false-positive results and enabling early disease detection.[21]

The versatility of Cas12a has allowed CRISPR-Cas12a-based systems to become a valuable tool for a wide range of diagnostic applications. Additionally, they have facilitated the development of user-friendly, point-of-care (POC) diagnostic platforms, offering several benefits over conventional methods, such as providing rapid results and enabling timely clinical decision-making cost-effectively.[22,23] While CRISPR-Cas systems have advanced molecular diagnostics of vector-borne viruses such as dengue and Zika virus, several limitations remain.[24,25] Factors such as target abundance and interference from the biological matrix may influence the detection limit. Optimising these factors is crucial to ensure reliable detection and enhance sensitivity and accuracy for achieving highly specific and sensitive detection of pathogens.[24–26]

This study presents a CRISPR-Cas12a-based WNV detection procedure, characterised by high specificity and sensitivity. Key parameters, including the concentrations of target DNA, Cas12a, crRNA, and fluorescent probe, as well as reaction duration and temperature, were systematically evaluated to maximise signal output and achieve efficient WNV detection. Additionally, an isothermal amplification method, reverse transcriptase recombinase polymerase amplification (RT-RPA), was integrated into this protocol to enhance sensitivity and lower the limit of detection (LOD) of the test system (Scheme 1). The method demonstrated the capacity to detect WNV at picomolar (pM) concentrations within one hour. This approach has the potential to facilitate widespread adoption of CRISPR-Cas12a-based sensors in diagnostic applications.

Results and discussion

### Validation of Cas12a target specificity and temporal dynamics

To initially validate Cas12a's catalytic activity and confirm its target specificity, a series of controlled experiments were performed (Fig. 1). The analysis included Human *HPRT1* utilising a corresponding specific crRNA, which served as a positive control, and the WNV *E* gene with its crRNA. Target specificity was assessed through the inclusion of a negative control crRNA in both reactions.

The data demonstrated a notable difference in relative fluorescence units (RFUs) between assays employing negative crRNA or target-specific crRNAs. *HPRT1* and WNV crRNAs elicited RFU values exceeding 500, whereas negative control crRNAs yielded RFU levels less than 100, thus corroborating the system's specificity and sensitivity (Fig. 1A). Another analysis was subsequently conducted to characterise the temporal dynamics of Cas12a activity. RFU levels were quantified at discrete time intervals (0, 10, 20, 30, 40, 50, and 60 min) in reactions containing the *HPRT1* DNA. The data demonstrated a rapid increase in RFU levels, with a detectable signal observed within the first minutes of reaction initiation. Following this
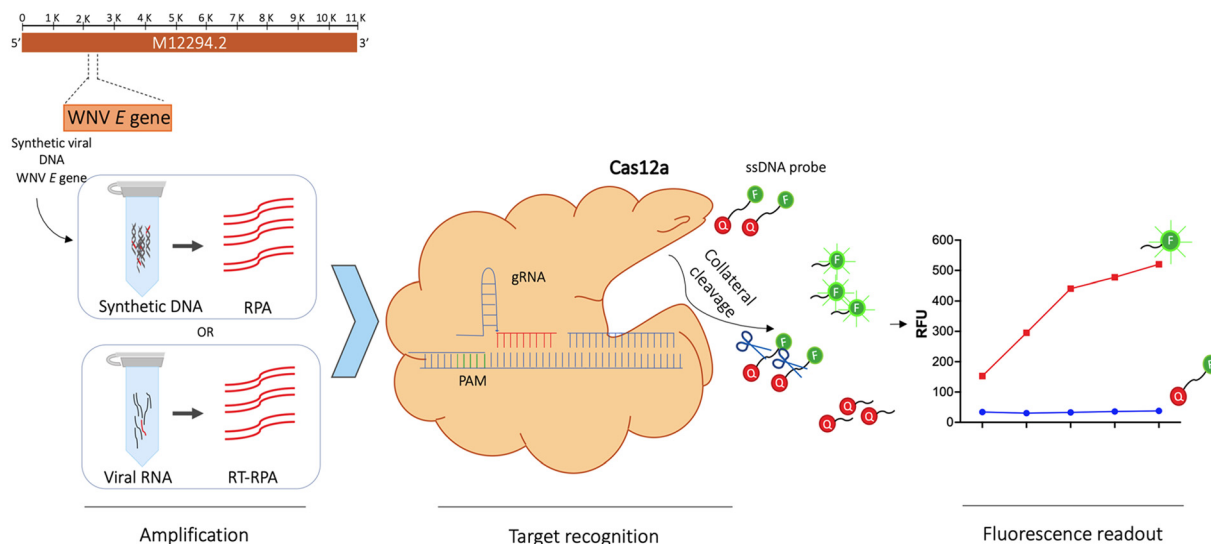
Scheme 1 Workflow of the CRISPR-Cas12a-based WNV detection assay. The study involved targeting the gene encoding WNV envelope protein (WNV *E* gene) for specific detection. Synthetic 500 bp WNV DNA and isolated WNV RNA served as templates for isothermal amplification *via* RPA and RT-RPA, respectively. The amplified products were then subjected to Cas12a-mediated target recognition, with target detection confirmed through the fluorescence signal readout.
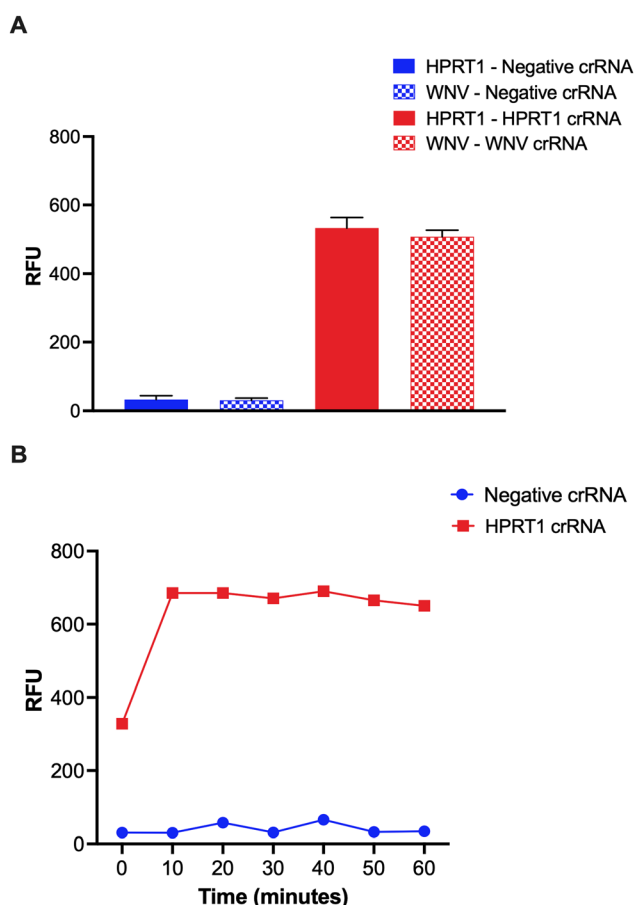
Fig. 1 Verification of the Cas12a's ability to cleave target DNA. (A) Target-specific cleavage activity of Cas12a was confirmed using crRNAs targeting human *HPRT1* and WNV *E* genes, along with a negative control. (B) A time-course analysis revealed a rapid and efficient cleavage of *HPRT1* DNA by Cas12a, with detectable activity starting at t = 0.

initial increase, RFU values reached a plateau of approximately 700 by 10 minutes, which was maintained throughout the remaining time course (Fig. 1B). In contrast, reactions containing a negative control crRNA exhibited consistently low RFU values. Collectively, these findings provide compelling evidence for Cas12a's ability to efficiently and specifically cleave diverse target DNA sequences in a relatively short period.
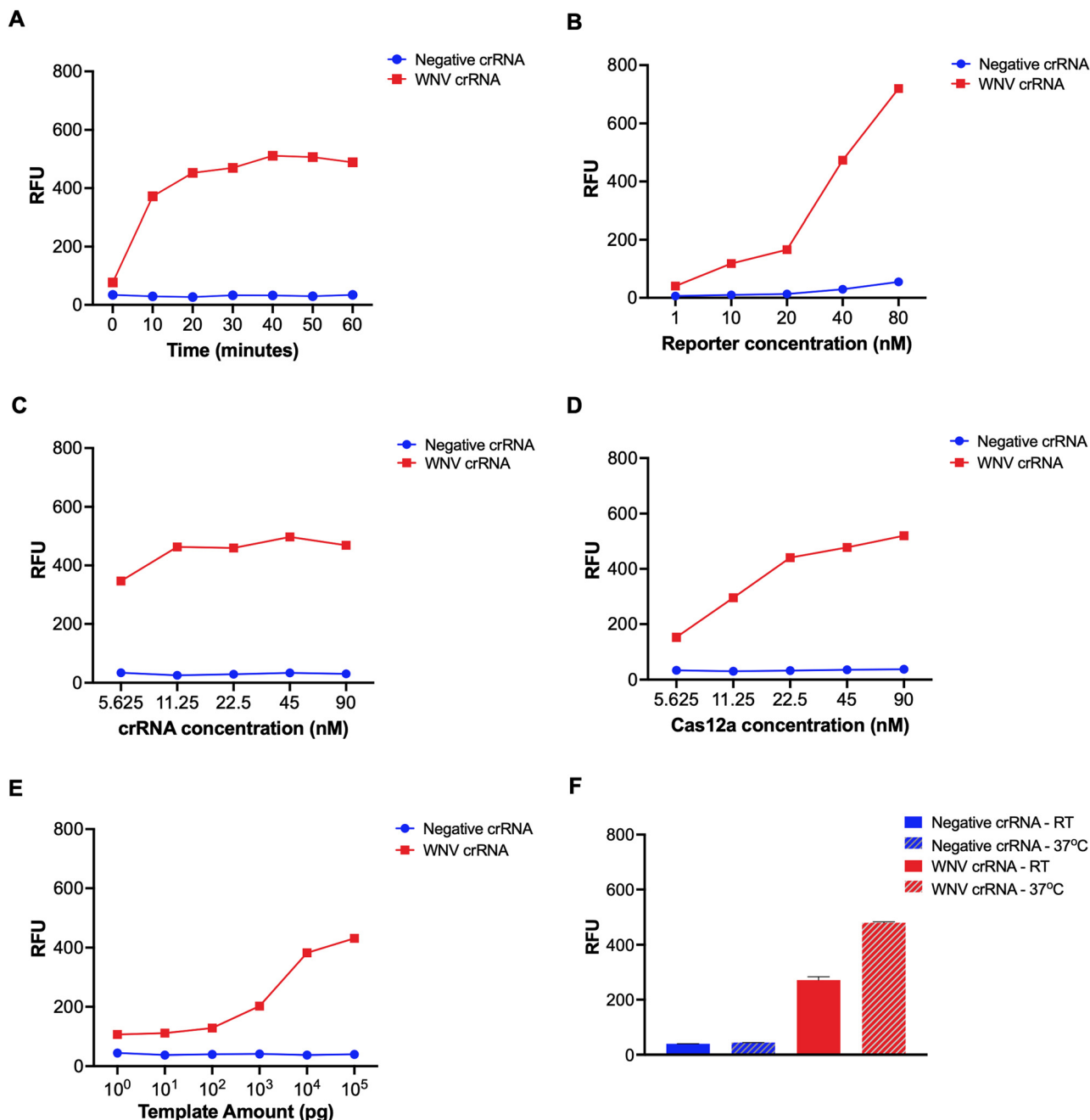
Systematic optimisation of Cas12a-mediated WNV detection

Next, a comprehensive analysis was conducted by testing different parameters to achieve maximal signal output, quantified as RFUs (Fig. 2). This analysis focused on the evaluation of temporal dynamics of the Cas12a and the concentration of key reaction constituents, specifically: reaction incubation time (Fig. 2A), reporter concentration (Fig. 2B), crRNA concentration (Fig. 2C), Cas12a concentration (Fig. 2D), and template DNA concentration (Fig. 2E). Furthermore, the robustness of the assay was assessed by evaluating its performance at both room temperature (RT) and 37 °C, thereby investigating its potential for use in resource-limited settings where precise temperature control may be challenging (Fig. 2F).

In terms of temporal dynamics, the WNV reaction yielded similar results to those observed with HPRT1, illustrated in Fig. 1B, with a few differences. A detectable RFU value was observed at around 3 min, although to a lesser extent than *HPRT1* since RFU levels were approximately 100 and 300 for WNV *E* and *HPRT1*, respectively. Signal in the WNV reaction reached 400 at 10 min, and reached a plateau after 20 min (Fig. 2A). A maximum signal was observed at 40 min in both reactions. To facilitate a rapid procedural workflow, 30 minutes was determined as the optimal duration for the subsequent analyses.

Another aim of this study was to optimise the Cas12a-based WNV detection system by minimising reagent concentrations

Fig. 2 Systematic optimisation of the Cas12a-mediated detection of the WNV. Various parameters, such as (A) time and concentrations of (B) reporter, (C) crRNA, (D) Cas12a, and (E) template DNA, were tested to achieve the maximal fluorescence signal output, quantified as RFUs. (F) The reactions were also run at room temperature (RT) and 37 °C to test the adaptability of the test system to different environments. The standard reaction mixture consisted of 45 nM Cas12a, 45 nM crRNA, 40 nM reporter, and 100 ng of template DNA, unless otherwise stated.

while preserving assay sensitivity, a crucial factor for reducing the economic burden of Cas-based diagnostics. To this end, the impact of varying reagent concentrations on the signal output was assessed. A near-linear relationship between the RFU and both the reporter concentration (Fig. 2B) and template DNA amount was observed (Fig. 2E). The limit of detection was established at 10 nM reporter concentration, while template DNA concentrations ranging from 1 to 100 pg (corresponding to 0.15–15 pM) yielded comparable and reliable signal outputs.

Notably, crRNA and Cas12a concentrations exhibited a weaker correlation with RFUs (Fig. 2C and D). This observation aligns with the established mechanism of Cas12a activation, where a complex of crRNA and Cas12a is essential for target recognition and subsequent collateral activity.[27] Thus, these results support previous findings that maintaining a 1 : 1 crRNA : Cas12a ratio appears to be critical for optimal assay performance,[28] since increasing either component independently does not substantially enhance the signal output. Furthermore, while 37 °C

represents the optimal reaction temperature, reliable signal detection was confirmed at ambient temperature (Fig. 2F). The data demonstrate the system's robustness, as evidenced by negligible RFUs in negative crRNA controls, and its capacity to detect WNV with high specificity and sensitivity.

Confirmation of Cas12a-mediated cleavage of template DNA

To validate the *cis*-cleavage activity of CRISPR-Cas12a on template DNA, agarose gel electrophoresis was performed (Fig. 3). Specificity was established by comparing reactions using a negative control and WNV-specific crRNA on the WNV template (Fig. 3A). The absence of cleavage products in the negative control (lane #4), as opposed to the presence of the expected two bands (uncleaved template of 430 bp and the longer cleavage product of 276 bp) in the WNV-specific crRNA reaction (lane #6), confirmed the system's specificity.

Interestingly, we did not observe the second cleavage product of 154 bp on the gel. The diminished intensity of this product potentially results from ongoing, non-specific Cas12a activity, leading to the degradation of smaller DNA fragments.[29] While template cleavage was not complete, this did not substantially compromise signal intensity, as evidenced by RFU values of 913.5 and 73.7 for the WNV-specific and negative control crRNA reactions, respectively (data not shown). To completely cleave the template DNA, reaction component concentrations were increased (Cas12a: 225 nM, crRNA: 225 nM, reporter: 200 nM, template DNA: 250 ng (37.5 nM)), and the cleavage profile of Cas12a was assessed. This resulted in a substantial increase in the cleaved : uncleaved template DNA ratio, as evidenced by agarose gel electrophoresis (Fig. 3B). Furthermore, the inclusion of reporters in a subset of these reactions allowed for the assessment of their potential influence on Cas12a cleavage activity. The analysis revealed that the presence of reporters did not significantly alter the observed band patterns, suggesting a negligible, if any, effect on the cleavage process (Fig. 3B).

Optimisation of reverse transcriptase recombinase polymerase amplification (RT-RPA)

The results presented so far were obtained by using synthetic DNA purchased from IDT (New Jersey, US), corresponding to the WNV *E* gene fragment. The pre-amplification of this fragment was performed by traditional PCR. However, the requirement for a thermal cycler in PCR does not adhere to the ASSURED criteria (affordable, sensitive, specific, user-friendly, rapid, equipment-free, and deliverable) essential for point-of-care (POC) applications, thereby restricting its use in such settings.[30] To make our method of CRISPR-Cas12a-based WNV detection applicable to POC platforms, we employed a faster and simpler isothermal pre-amplification technique, reverse transcriptase recombinase polymerase amplification (RT-RPA), eliminating the need for expensive and complex thermal cycling equipment. RT-RPA, despite its distinct amplification mechanism from RT-PCR, consistently demonstrates comparable or even superior detection sensitivity and speed across various pathogens, including canine distemper (CDV), cassava brown streak (CBSV), murine hepatitis (MHV), and severe acute respiratory syndrome
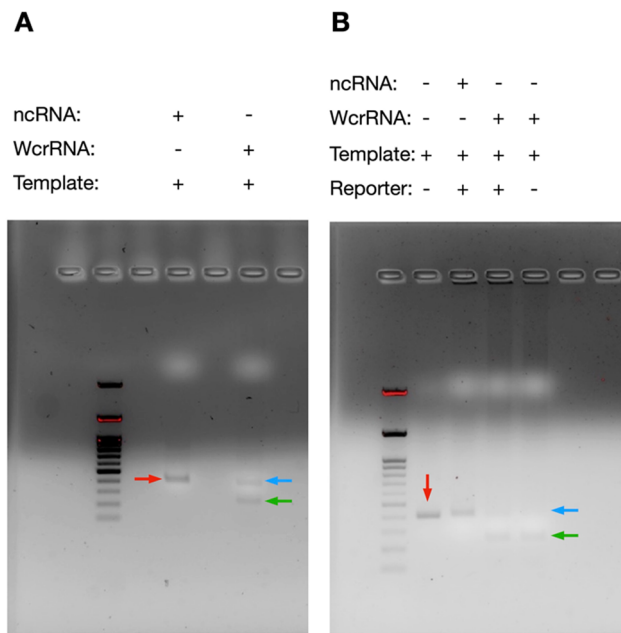

Fig. 3 CRISPR/Cas12a reactions run on a 1.5% agarose gel. (A) WNV DNA was used as a template in Cas12a reactions with negative (ncrRNA) or WNV-specific crRNA (WcrRNA). The reaction mixtures consisted of 90 nM Cas12a, 90 nM crRNA, 80 nM reporter, and 100 ng (15 nM) of template DNA. (B) WNV DNA was either run directly on the gel or used as a template in Cas12a reactions with ncrRNA or WcrRNA, with or without reporter. The reaction mixtures consisted of 225 nM Cas12a, 225 nM crRNA, 200 nM reporter, and 250 ng of template DNA. Red arrows represent 430 bp template DNA alone, whereas blue and green arrows show 430 bp uncut DNA and 276 bp CRISPR-Cas12a reaction product, respectively.

coronavirus 2 (SARS-CoV-2) viruses.[31–34] While the detection limit of RT-RPA varied across studies (*e.g.*, 31.8 copies for CDV,[31] 10^{-5} for CBSV,[32] 4.45×10^1 copies per μL for MHV,[33] and 1–3 copies for SARS-CoV-2),[34] the high sensitivity and short reaction times (under 30 min) were maintained. In the current study, RT-RPA was utilised due to its comparable sensitivity to RT-PCR, and combined with Cas12a for target detection.

For this purpose, viral RNA isolated from WNV or synthetic WNV DNA was used as an initial template in the RT-RPA and RPA reactions, respectively (Fig. 4). To evaluate the system's efficiency and specificity, multiple reactions were prepared. Both RPA (lane #2) and RT-RPA (lane #3) reactions containing the positive control (lane #1), provided within the RT-RPA kit, produced bands of the expected size (143 bp). The third reaction was specifically performed to ensure that reverse transcriptase did not compromise the amplification efficiency (Fig. 4A). Subsequently, the RPA system's efficacy was validated using synthetic WNV DNA as input. A substantial increase in band intensity was observed in the RPA reaction (lane #6) compared to its starting material, *i.e.* 100 ng (15 nM) of WNV synthetic DNA (lane #5). Finally, WNV RNA was introduced into RT-RPA reactions and incubated for 30 (lane #7) or 60 (lane #8) min. Both time points resulted in bands of the predicted size (430 bp), with the 60-minute reaction producing a higher amplicon yield as indicated by an increased band intensity (Fig. 4A).
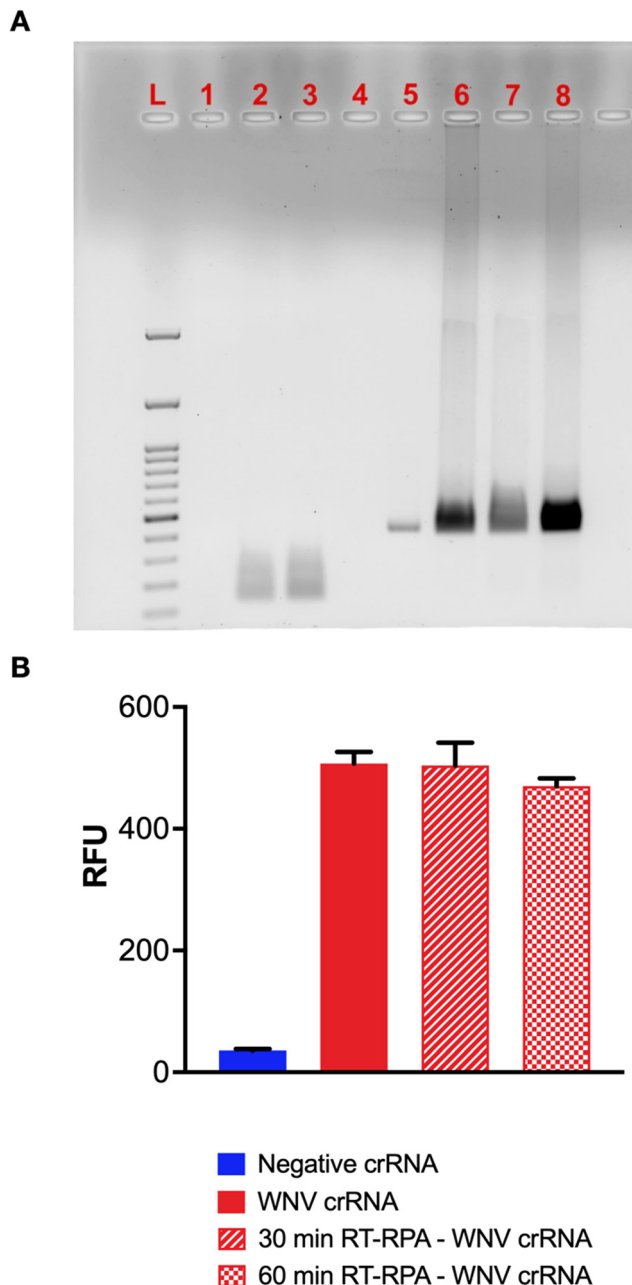
Fig. 4 Optimisation of the RT-RPA reaction and isothermal amplification of the target sequence. (A) RPA and RT-RPA reactions were run with a positive control supplied with the TwistAmp® kit, synthetic WNV DNA or WNV RNA. Reactions were as follows: (1) positive control DNA or template, (2) RPA with positive control, (3) RT-RPA with positive control, (4) blank, (5) 100 ng (15 nM) of WNV synthetic DNA, (6) RPA on WNV synthetic DNA, (7) RT-RPA on WNV RNA for 30 min, and (8) RT-RPA on RNA for 60 min. L: DNA ladder. (B) RFU values obtained from the RT-RPA followed by CRISPR-Cas12a reactions run for 30 or 60 min, or CRISPR-Cas12a reactions alone using either negative crRNA or WNV crRNA with synthetic DNA.

Following the confirmation of target amplification *via* RT-RPA, downstream CRISPR-Cas12a detection assays were performed on the resulting amplicons (Fig. 4B). Reactions containing synthetic WNV DNA or RT-RPA products derived from WNV RNA yielded comparable results, as indicated by RFU values.

Notably, the duration of the RT-RPA reaction did not significantly impact the average RFU values obtained in the CRISPR-Cas12a assay, suggesting that shorter RT-RPA incubation times were sufficient to generate a detectable signal. Together, these findings demonstrate that our two-step approach involving pre-amplification of WNV RNA with RT-RPA followed by CRISPR-Cas12a-based detection is a reliable, highly sensitive and specific assay that could be performed within one hour utilising authentic viral RNA.

Assessing the performance of the WNV detection assay in simulated biological matrices

As the final step of the methodological framework, this study aimed to validate the efficacy of our detection protocol in the presence of the host genomic material. Given the global health implications of WNV, which induces severe neurological conditions in humans and is primarily transmitted by *Culex* spp., genetic materials extracted from both human and mosquito were employed as background matrices. To simulate authentic samples obtained in a POC setting, human or fly DNA was combined with the amplified products of RPA and RT-RPA reactions conducted using synthetic WNV DNA or genuine WNV RNA templates, respectively (Fig. 5).

The findings revealed that the RPA product generated a robust fluorescent signal, while human DNA alone did not elicit a notable RFU signal with the WNV-specific crRNA (Fig. 5A).

Furthermore, the inclusion of human DNA in the RT-RPA product did not significantly hinder the fluorescent signal. Similarly, mosquito DNA yielded an RFU value below 100 with the WNV crRNA, which was established as the detection threshold in matrix experiments (Fig. 5B). The RPA product produced an RFU value of approximately 450, and the RT-RPA product generated a strong fluorescent signal (app. 600) even with the addition of mosquito DNA. The incorporation of mosquito DNA resulted in a negligible increase of approximately 10% in the RFU signal.

Finally, to establish the limit of detection for the CRISPR-Cas12a-based detection protocol coupled with RT-RPA, a broad range of initial WNV genetic material concentrations (10^{-2} pg to 10^{5} pg) was tested. The fluorescent signals obtained from these reactions were consistently high (approximately 600 RFUs) and similar to those observed in the positive control reaction containing synthetic WNV DNA (Fig. 5C). This indicates that RPA functions with remarkable efficiency even with a minute amount of starting material. Interestingly, no linear relationship was observed between WNV RNA concentration and RFU levels. This suggests that even at concentrations as low as 10^{-2} pg, the viral RNA was sufficiently amplified by RT-RPA to cleave all FAM-BHQ reporters, leading to signal saturation. Therefore, higher WNV RNA concentrations did not yield proportionally higher RFU levels. Agarose gel electrophoresis further confirmed the relatively similar amount of amplified products across these concentrations (Fig. 5D). These results demonstrated that our diagnostic protocol exhibited the capacity to detect WNV with high specificity and sensitivity, and across diverse scenarios, including the presence of distinct host genetic backgrounds and low viral loads.
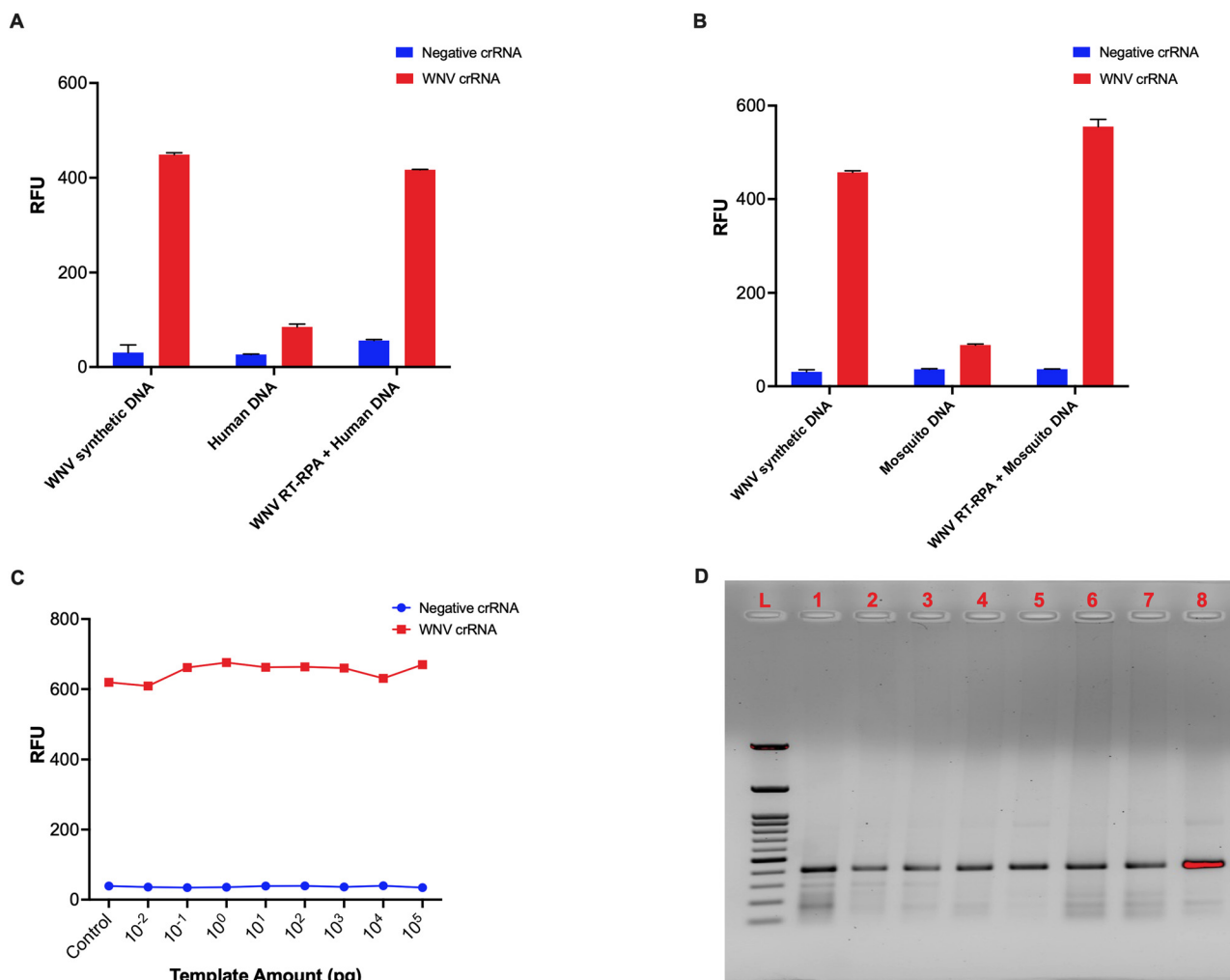
Fig. 5 Validation of the WNV detection in biological matrices and testing the LOD of the diagnostic system. Cas12a-mediated cleavage assays were performed using 100 ng of synthetic WNV DNA, human DNA (A) or *Culex* DNA (B) alone, or a combination of human or fly DNA and 100 ng of WNV RT-RPA product, with either a negative control crRNA or a WNV-specific crRNA. LOD analysis for the RT-RPA + CRISPR-Cas12a protocol was performed with (C) different concentrations of the initial WNV genetic material. (D) Agarose gel electrophoresis of reaction products. L: DNA ladder. Lanes 1–8: CRISPR-Cas12a reactions with WNV RNA concentrations from 10^5 to 10^{-2} pg, decreasing tenfold per lane.

Future research should focus on validating the system's performance in POC settings using samples from active or passive surveillance studies of vectors and/or hosts.

Experimental

Virus preparation and viral RNA extraction

Vero cells were cultured in Dulbecco's modified Eagle medium (DMEM) supplemented with 10% fetal bovine serum and 1% penicillin–streptomycin. The cells were allowed to grow for one day. A working solution of WNV was prepared through the reconstitution of a frozen viral stock derived from prior studies[35,36] and cells were infected with the virus in DMEM. After four days of incubation under standard conditions (37 °C, 5% CO_2), the culture media were collected and centrifuged at 3000 rpm for 15 min at 4 °C. The supernatant containing the virus particles was collected. The virus titer was determined to be $10^{5.75}/0.1$ ml using the TCID50 assay. A stock solution was

prepared from the supernatant and inactivated by heat (at 56 °C for 30 minutes). The stocks were stored at −80 °C until RNA extraction. WNV total RNA was extracted using High Pure RNA Isolation Kit (Roche) according to the manufacturer's guidelines.

Isolation of *Culex pipiens* s.l. DNA

Genomic DNA was isolated from the thoracic tissue of individual specimens using the Qiagen DNeasy Blood and Tissue Kit (Hilden, Germany) following the manufacturer's guidelines. An overnight incubation at 56 °C was performed for Proteinase K-mediated lysis, following a protocol described in a previous study.[37] Extracted DNA samples were maintained at −20 °C until further analysis.

CRISPR-Cas12a system design

The CRISPR-Cas12a system was chosen for WNV detection based on its distinct advantages compared to other

CRISPR-Cas systems. Notably, while Cas9 and Cas12 primarily target double-stranded DNA, and Cas13 targets single-stranded RNA, the DNA specificity of Cas12a enables the pre-amplification of the target oligonucleotide. This strategy offers a significant signal enhancement, resulting in high sensitivity and a low limit of detection (LOD). Furthermore, the inherent DNA recognition of Cas12a, in contrast to the RNA-targeting Cas13, eliminates the necessity for an additional transcription step (*i.e.*, RNA synthesis from DNA) prior to target recognition, thereby simplifying the overall protocol.[38]

The non-specific cleavage of nucleic acids following target recognition is defined as the collateral cleavage or *trans*-cleavage activity. Cas12a exhibits *trans*-cleavage activity against single-stranded DNA (ssDNA) and Cas13 demonstrates this activity against single-stranded RNA (ssRNA). In contrast, the collateral cleavage activity of Cas9 is considerably less pronounced. The ability of Cas12 to cleave ssDNA has been widely adopted for diagnostic applications.[27,39,40] Consequently, the CRISPR-Cas12a system was selected to detect WNV in this study.

Target selection and crRNA design. The CRISPR/Cas12a-based WNV detection exploits the enzyme's non-specific *trans*-cleavage activity. Following crRNA-guided complex formation, target recognition and Cas12a activation, this *trans*-cleavage activity results in the cleavage of reporter molecules, generating a fluorescent signal.[19,20] The target sequence on the WNV genome was selected based on specificity to WNV and possession of a PAM sequence (TTTV). For optimisation experiments, synthetic DNA composed of a 500 bp WNV envelope glycoprotein *E* gene (referred to as WNV *E* gene throughout the manuscript) fragment was purchased from IDT (New Jersey, US). The location of the target sequence on the WNV genome is shown in Scheme 1. Human *HPRT1* gene fragment and *HPRT1*-specific crRNA, purchased from IDT, were used as positive controls. A fluorescent reporter containing FAM was also purchased from IDT. Sequence information of the positive and negative crRNAs, reporter, and primers is provided in Table 1.

Primer design. Primers for the pre-amplification were designed using Primer-BLAST with default parameters, targeting amplicon lengths of approximately 460 bp for WNV *E* and 744 bp for *HPRT1*, encompassing the Cas12a PAM sequence. The same forward and reverse primers (Table 1) were used for WNV DNA amplification *via* both polymerase chain reaction (PCR), recombinase polymerase amplification (RPA), and RT-RPA. Primers were purchased from Sentebiolab Biotech (Ankara, Türkiye). Amplicons containing target sequences

on the WNV genome and human *HPRT1* gene are given in Table 2.

Amplification of the target regions

PCR. PCR reactions for the synthetic WNV DNA and human *HPRT1* gene fragment were carried out with a DreamTaq PCR Master Mix (2X) (Thermo Scientific, US) according to the manufacturer's instructions. The reaction volumes were adjusted to 50 μL with primer concentrations of 0.25 μM and 100 ng of DNA. PCR reactions were performed on a T100 Thermal Cycler (Biorad, US). The optimum annealing temperatures were determined by running reactions with increasing annealing temperatures from 57 °C to 63 °C. The conditions for the PCR protocol used with the primers listed in Table 1 were 95 °C for 3 min, 35 cycles of (95 °C for 30 s, 61 °C for 30 s, and 72 °C for 1 min), 72 °C for 10 min and cooling to 4 °C. PCR products were separated on 1.5% agarose gels in 1X TAE buffer with gel electrophoresis, and visualised using a ChemiDoc MP Imaging System (Biorad, US).

RT-RPA and RPA. Viral RNA, extracted from WNV-infected Vero cells, served as the template for the RT-RPA reaction. Following the manufacturer's protocol, reverse transcription was performed using RevertAid Reverse Transcriptase (Thermo Scientific, US). RPA reactions were conducted utilising a TwistAmp® Liquid Basic Kit (TABAS03KIT, TwistDx, Maidenhead, UK) according to the manufacturer's instructions. Each 50 μL reaction comprised 10 μM of each primer, 150 U of reverse transcriptase, 29.5 μL of rehydration buffer, 2.5 μL of 280 mM MgOAc, and 1 μg of template RNA. Reaction optimisation was performed at 37 °C. As a control, parallel RPA reactions were prepared following an identical protocol, with the exclusion of reverse transcriptase and the substitution of the RNA template with 100 ng of DNA. Prior to separation on 1.5% agarose gels in 1X TAE buffer, amplicons were purified using a PureLink Quick PCR Purification Kit (Invitrogen, US).

CRISPR-Cas12a assay

Upon the amplification of the target DNA, CRISPR-Cas12a reactions were prepared using different concentrations of reporter, crRNA, Cas12a, target DNA, and at different conditions (temperature and duration). Optimum conditions were selected based on the results of these experiments. Initially, the human *HPRT1* gene fragment and *HPRT1* crRNA were used as a positive control to validate the functionality of the assay. Subsequent experiments performed with WNV DNA and crRNA included a negative crRNA to ensure the specificity of the reaction. Standard reactions were prepared using 45 nM L.b. Cas12a (Cpf1), 45 nM crRNA, and 40 nM FAM-BHQ reporter, all purchased from IDT (New Jersey, US), 10X NEBuffer r2.1 (NEB, Massachusetts, US), 100 ng of DNA, and nuclease-free water (Sigma-Aldrich, US) to adjust the volume to 30 μL. The resulting RFU values were recorded using a Nanodrop 3300 (Thermo Scientific, US).

Matrix experiments

To simulate authentic biological conditions and evaluate the system's capacity for WNV genetic material detection amidst

Table 1 Sequences of the crRNAs, reporter, and PCR primers

Name	Sequence (5′ → 3′)
HPRT1 crRNA	GGTTAAAGATGGTTAAATGAT
WNV *E* crRNA	GAGGGATGTCCTGGATCACACAGG
Negative crRNA	CGTTAATCGCGTATAATACGG
HPRT1 – forward	ACCATGGTACACTCAGCACGGATG
HPRT1 – reverse	CCAGAGTAAGAGGCAGGTATTCAA
WNV *E*– forward	CACACTCAGAGGAGCTCAACGA
WNV *E*– reverse	TTCTGCATGTGCTTTCTGGATAAT
Reporter	56-FAM/TCGTATCCAGTGCGAATCACTC/3BHQ_1

Table 2 Target sequences on the human *HPRT1* gene and WNV *E* gene fragments

Target name	Sequence (5′ → 3′)
Human *HPRT1* (Ref: NG_012329.2)	TCACCTCTCCCACACCCTTTTATAGTTTAGGGATTGTATT TCCAAGGTTTCTAGACTGAGAGCCCTTTTCATCTTTGCTC ATTGACACTCTGTACCCATTAATCCTCCTTATTAGCTCCC CTTCAATGGACACATGGGTAGTCAGGGTGCAGGTCTCA GAACTGTCCTTCAGGTTCCAGGTGATCAACCAAGTGCCT TGTCTGTAGTGTCAACTCATTGCTGCCCCTTCCTAGTAAT CCCCATAATTTAGCTCTCCATTTCATAGTCTTTCCTTGGG TGTGTTAAAAGTGACCATGGTACACTCAGCACGGATGA AATGAAACAGTGTTTAGAAACGTCAGTCTTCTCTTTTGT AATGCCCTGTAGTCTCTCTGTATGTTATATGTCACATTTT GTAATTAACAGCTTGCTGGTGAAAAGGACCCCACGAAG TGTTGGATATAAGCCAGACTGTAAGTGAATTACTTTTTT TGTCAATCATTTAACCATCTTTAACCTAAAAGAGTTTTAT GTGAAATGGCTTATAATTGCTTAGAGAATATTTGTAGAG AGGCACATTTGCCAGTATTAGATTTAAAAGTGATGTTTT CTTTATCTAAATGATGAATTATGATTCTTTTTAGTTGTTG GATTTGAAATTCCAGACAAGTTTGTTGTAGGATATGCCC TTGACTATAATGAATACTTCAGGGATTTGAATGTAAGTA ATTGCTTCTTTTTCTCACTCATTTTTCAAAACACGCATAAA AATTTAGGAAAGAGAATTGTTTCTCCTTCCAGCACCTC ATAAATTTGAACAGACTGATGGTTCCCATTAGTCACATAA AGCTGTAGTCTAGTACAGACGTCCTTAGAACTGGAACCT GGCCAGGCTAGGGTGACACTTCTTGTTGGCTGAAATAG TTGAACAGCTTTAATATACAATAATTGTTGCATTATTATT TCAGATGATAAATGTGGTCATAAGTAAGAAATAAATGA TCGAGTTTAGTCTTTTAATTCACTGTCCTTTGAATACCTG CCTCTTACTCTGGAGGCAGAAGTCCCATGGATGTGTTTA TGAACATGGTTGAGGAAGATTTAGGAAGACTGCAACAG TACACTACCTAAAGCAGGTTTTTTACTCCATCTTTTTTTG CCACGTACACTGGCCTCCCACTTTGATATGCTTGAAATTA TCTCCTTGATTTGTCTTTCAAAACTACATATTGAGGCTGG TTGCGGTGGCTCACACCTGTAATCCTAGCACTTTGGG
WNV (Ref: M12294.2)	TACCACCACACTCAGAGGAGCTCAACGACTCGCAGCTCT TGGAGATACTGCTTGGGATTTTGGATCAGTTGGAGGGG TTTTCACCTCAGTGGGGAAAGCCATACACCAAGTCTTTG GAGGAGCTTTTAGATCACTCTTTGGAGGGATGTCCTGG ATCACACAGGGACTTCTGGGAGCTCTTCTGTTGTGGATG GGAATCAATGCCCGTGACAGGTCAATTGCTATGACGTTT CTTGCGGTTGGAGGAGTTTTGCTCTTCCTTTCGGTCAAC GTCCATGCTGACACAGGCGTGTGCCATTGATATTGGCAG GCAAGAGCTCCGGTGCGGAAGTGGAGTGTTTATCCACA ACGATGTGGAAGCCTGGATGGATCGTTACAAGTTCTAC CCGGAGACGCCACAGGGCCTAGCAAAAATTATCCAGAA AGCACATGCAGAAGGAGTCTGCGGCTTGCGTTCCGTTT CCAGACTCGAGCACCAAATGTGGGAAGCCATTAAGGAT G

The red and green letters refer to the sequences recognised by forward and reverse primers, and target-specific crRNA, respectively.

host nucleic acids, matrix experiments were conducted employing *Culex pipiens* s.l. or human DNA samples as background matrices. RPA and RT-RPA reaction products were subjected to purification utilising a PureLink Quick PCR Purification Kit. Upon purification, reactions for the Cas12a assay comprised 100 ng of background DNA (mosquito or human) combined with 100 ng of either synthetic WNV DNA or WNV RT-RPA product, following the standard Cas12a protocol. The resulting reaction products were analysed by 1.5% agarose gel electrophoresis or quantified by recording RFUs using a NanoDrop 3300 spectrophotometer. Dr Baran Erman (Institute of Child Health, Hacettepe University, Ankara, Türkiye) kindly provided human DNA samples.

Data visualisation

Data were visualised using GraphPad Prism Version 9 (California, US). Scheme 1 was drawn using PowerPoint 2021 (Microsoft, US). Data are presented as mean + standard deviation for bar graphs, and as mean for line graphs. For each parameter tested, three independent measurements were recorded.

Conclusions

This study successfully developed a rapid, highly specific, and sensitive CRISPR-Cas12a-based assay for WNV detection, achieving 10 fM sensitivity within one hour through integration with RT-RPA. The integration of RT-RPA significantly lowered the detection limit from 1 ng to 10 fg of target, corresponding to 2.15×10^9 DNA copies and 1.77×10^3 RNA copies, respectively. Key reaction parameters, including duration, temperature, and reaction constituent concentrations, were also systematically optimised. Our data suggest that reporter and template amounts are critical limiting factors for fluorescence signal levels. Therefore, future studies involving CRISPR/Cas12a-based molecular detection should prioritise these factors during optimisation. The assay's functionality at ambient temperatures and with the host genetic material indicates its significant potential for use in POC settings, addressing current limitations in WNV diagnostics. Furthermore, the modular nature of the CRISPR-Cas system and the isothermal amplification strategy employed suggest a strong adaptability of this approach for the detection of other vector-borne diseases and their associated pathogens. By simply redesigning the guide RNA to target specific nucleic acid sequences of different pathogens transmitted by vectors such as mosquitoes, ticks, or sandflies, this platform could be readily tailored for the rapid and decentralised diagnosis of other vector-borne diseases. These characteristics hold considerable promise for enhancing global surveillance efforts and enabling timely interventions against the growing threat of vector-borne diseases.

Ethics statement

All experiments were performed following the guidelines of the Turkish legislation and Hacettepe University, and complied with the regulations of the Institutional Ethics Committee of Hacettepe University, Ankara, Türkiye.

Author contributions

Asli Erol: investigation, methodology, validation, data curation, formal analysis, and writing – original draft. Dilan

Conflicts of interest

There are no conflicts to declare.

Data availability

The gel images included in this manuscript have been globally enhanced to optimise their visual clarity. These adjustments were applied uniformly across the entire image. The original, raw data are available upon reasonable request.

Acknowledgements

References

1 World Health Organization, https://www.who.int/news-room/fact-sheets/detail/vector-borne-diseases, (accessed January 2025).

2 J. Lourenço, S. C. Barros, L. Zé-Zé, D. S. C. Damineli, M. Giovanetti, H. C. Osório, F. Amaro, A. M. Henriques, F. Ramos, T. Luís, M. D. Duarte, T. Fagulha, M. J. Alves and U. Obolski, *Commun. Biol.*, 2022, **5**(1), 6, DOI: 10.1038/s42003-021-02969-3.

3 U.S. Centers for Disease Control and Prevention, https://www.cdc.gov/climate-health/php/effects/vectors.html#:~:text=Climate%20is%20one%20of%20the,risk%20for%20vector%2Dborne%20infections., (accessed January 2025).

4 C. Caminade, K. M. McIntyre and A. E. Jones, *Ann. N. Y. Acad. Sci.*, 2019, **1436**(1), 157–173, DOI: 10.1111/nyas.13950.

5 G. Habarugira, W. W. Suen, J. Hobson-Peters, R. A. Hall and H. Bielefeldt-Ohmann, *Pathogens*, 2020, **9**, 589, DOI: 10.3390/pathogens9070589.

6 J. C. Saiz, M. A. Martín-Acebes, A. B. Blázquez, E. Escribano-Romero, T. Poderoso and N. Jiménez de Oya, *Virulence*, 2021, **12**(1), 1145–1173, DOI: 10.1080/21505594.2021.1908740.

7 D. Erazo, L. Grant, G. Ghisbain, G. Marini, F. J. Colón-González, W. Wint, A. Rizzoli, W. Van Bortel, C. B. F. Vogels, N. D. Grubaugh, M. Mengel, K. Frieler, W. Thiery and S. Dellicour, *Nat. Commun.*, 2024, **15**(1), 1196, DOI: 10.1038/s41467-024-45290-3.

8 F. J. May, C. T. Davis, R. B. Tesh and A. D. Barrett, *J. Virol.*, 2011, **85**, 2964–2974, DOI: 10.1128/JVI.01963-10.

9 T. Vilibic-Cavlek, M. Bogdanic, V. Savic, Z. Hruskar, L. Barbic, V. Stevanovic, L. Antolasic, L. Milasincic, D. Sabadi, G. Miletic, I. Coric, A. Mrzljak, E. Listes and G. Savini, *World J. Virol.*, 2024, **13**(4), 95986, DOI: 10.5501/wjv.v13.i4.95986.

10 S. A. Kemmerly, *Ochsner J*, 2003, **5**(3), 16–17.

11 A. A. Marfin and D. J. Gubler, *Clin. Infect. Dis.*, 2001, **33**, 1713–1719, DOI: 10.1086/322700.

12 I. H. Cvjetković, J. Radovanov, G. Kovačević, V. Turkulov and A. Patić, *Diagn. Microbiol. Infect. Dis.*, 2023, **107**(1), 115920, DOI: 10.1016/j.diagmicrobio.2023.115920.

13 G. Habarugira, W. W. Suen, J. Hobson-Peters, R. A. Hall and H. Bielefeldt-Ohmann, *Pathogens*, 2020, **9**(7), 589, DOI: 10.3390/pathogens9070589.

14 P. Y. Shi, E. B. Kauffman, P. Ren, A. Felton, J. H. Tai, A. P. 2nd Dupuis, S. A. Jones, K. A. Ngo, D. C. Nicholas, J. Maffei, G. D. Ebel, K. A. Bernard and L. D. Kramer, *J. Clin. Microbiol.*, 2001, **39**(4), 1264–1271, DOI: 10.1128/JCM.39.4.1264-1271.2001.

15 Y. Lustig, D. Sofer, E. D. Bucris and E. Mendelson, *Front. Microbiol.*, 2018, **9**, 2421, DOI: 10.3389/fmicb.2018.02421.

16 B. Zetsche, J. S. Gootenberg, O. O. Abudayyeh, I. M. Slaymaker, K. S. Makarova, P. Essletzbichler, S. E. Volz, J. van der Oost Joung, A. Regev, E. V. Koonin and F. Zhang, *Cell*, 2015, **163**(3), 759–771, DOI: 10.1016/j.cell.2015.09.038.

17 B. P. Kleinstiver, S. Q. Tsai, M. S. Prew, N. T. Nguyen, M. M. Welch, J. M. Lopez, Z. R. McCaw, M. J. Aryee and J. K. Joung, *Nat. Biotechnol.*, 2016, **34**(8), 869–874, DOI: 10.1038/nbt.3620.

18 Y. Tang and Y. Fu, *Cell Biosci.*, 2018, **8**, 59, DOI: 10.1186/s13578-018-0255-x.

19 J. S. Chen, E. Ma, L. B. Harrington, M. Da Costa, X. Tian, J. M. Palefsky and J. A. Doudna, *Science*, 2018, **360**(6387), 436–439, DOI: 10.1126/science.aar6245.

20 W. Feng, H. Zhang and X. C. Le, *Anal. Chem.*, 2023, **95**(1), 206–217, DOI: 10.1021/acs.analchem.2c04555.

21 I. Strohkendl, F. A. Saifuddin, J. R. Rybarski, I. J. Finkelstein and R. Russell, *Mol. Cell*, 2018, **71**(5), 816–824.e3, DOI: 10.1016/j.molcel.2018.06.043.

22 Z. Chen, J. Li, T. Li, T. Fan, C. Meng, C. Li, J. Kang, L. Chai, Y. Hao, Y. Tang, O. A. Al-Hartomy, S. Wageh, A. G. Al-Sehemi, Z. Luo, J. Yu, Y. Shao, D. Li, S. Feng, W. J. Liu, Y. He, X. Ma, Z. Xie and H. Zhang, *Natl. Sci. Rev.*, 2022, **9**(8), nwac104, DOI: 10.1093/nsr/nwac104.

23 R. Lei, Y. Li, L. Li, J. Wang, Z. Cui, R. Ju, L. Jiang, X. Liao, P. Wu and X. Wang, *Front. Plant Sci.*, 2022, **13**, 976510, DOI: 10.3389/fpls.2022.976510.

24 J. Zhou, Z. Li, J. Seun Olajide and G. Wang, *Heliyon*, 2024, **10**(4), e26179, DOI: 10.1016/j.heliyon.2024.e26179.

25 M. Wang, H. Wang, K. Li, X. Li, X. Wang and Z. Wang, *Foods*, 2023, **12**(3), 477, DOI: 10.3390/foods12030477.

26 Y. Chen, R. Zhao, X. Hu and X. Wang, *Anal. Chim. Acta*, 2025, **1336**, 343295, DOI: 10.1016/j.aca.2024.343295.

27 J. Li, Y. Wang, B. Wang, J. Lou, P. Ni, Y. Jin, S. Chen, G. Duan and R. Zhang, *Diagnostics*, 2022, **12**(10), 2455, DOI: **10.3390/diagnostics12102455**.

28 Y. Zhang, Y. Cheng, H. Fang, N. Roberts, L. Zhang, C. A. Vakulskas, R. P. Niedz, J. N. Culver and Y. Qi, *Front. Genome Ed.*, 2022, **4**, 780238, DOI: **10.3389/fgeed.2022.780238**.

29 E. A. Nalefski, R. M. Kooistra, I. Parikh, S. Hedley, K. Rajaraman and D. Madan, *Nucleic Acids Res.*, 2024, **52**(8), 4502–4522, DOI: **10.1093/nar/gkae152**.

30 X. Qian, Q. Xu, C. J. Lyon and T. Y. Hu, *Lab Chip*, 2024, **24**(20), 4717–4740, DOI: **10.1039/d4lc00340c**.

31 J. Wang, J. Wang, R. Li, L. Liu and W. Yuan, *BMC Vet. Res.*, 2017, **13**(1), 241, DOI: **10.1186/s12917-017-1180-7**.

32 F. M. Munguti, D. C. Kilalo, H. K. Yegon, I. Macharia, S. E. Seal, A. W. Mwango'mbe, E. N. Nyaboga and G. Silva, *Sci. Rep.*, 2024, **14**(1), 12438, DOI: **10.1038/s41598-024-62249-y**.

33 X. Wang, X. Sui, Y. Ma, M. Li, X. Zhang, D. Fei and M. Ma, *Front. Microbiol.*, 2022, **13**, 1067694, DOI: **10.3389/fmicb.2022.1067694**.

34 L. G. Liang, M. J. Zhu, R. He, D. R. Shi, R. Luo, J. Ji, L. F. Cheng, X. Y. Lu, W. Lu, F. M. Liu, Z. G. Wu, N. P. Wu, H. Chen, Z. Chen and H. P. Yao, *J. Med. Virol.*, 2023, **95**(1), e28139, DOI: **10.1002/jmv.28139**.

35 K. Ergunay, N. Litzba, A. Brinkmann, F. Gunay, Y. Sarikaya, S. Kar, S. Orsten, K. Oter, C. Domingo, O. Erisoz Kasap, A. Ozkul, L. Mitchell, A. Nitsche, B. Alten and Y. M. Linton, *Parasit Vectors*, 2017, **10**(1), 149, DOI: **10.1186/s13071-017-2087-7**.

36 A. Ozkul, K. Ergunay, A. Koysuren, F. Alkan, E. M. Arsava, S. Tezcan, G. Emekdas, S. Hacioglu, M. Turan and D. Us, *Int. J. Infect. Dis.*, 2013, **17**(7), e546–51, DOI: **10.1016/j.ijid.2013.02.005**.

37 O. E. Kasap, V. Dvorak, J. Depaquit, B. Alten, J. Votypka and P. Volf, *Infect., Genet. Evol.*, 2015, **34**, 467–479, DOI: **10.1016/j.meegid.2015.05.025**.

38 S. Rahimi, S. R. Balusamy, H. Perumalsamy, A. Ståhlberg and I. Mijakovic, *Nucleic Acids Res.*, 2024, **52**(17), 10040–10067, DOI: **10.1093/nar/gkae736**.

39 A. Varble and L. A. Marraffini, *Trends Genet.*, 2019, **35**(6), 446–456, DOI: **10.1016/j.tig.2019.03.009**.

40 D. K. Sahel, G. Giriprasad, R. Jatyan, S. Guha, A. Korde, A. Mittal, S. Bhand and D. Chitkara, *RSC Adv.*, 2024, **14**(44), 32411–32435, DOI: **10.1039/d4ra04838e**.